J. W. Hurrell · M. P. Hoerling · A. S. Phillips · T. Xu

Twentieth century north atlantic climate change. Part I: assessing determinism

Abstract Boreal winter North Atlantic climate change since 1950 is well described by a trend in the leading spatial structure of variability, known as the North Atlantic Oscillation (NAO). Through diagnoses of ensembles of atmospheric general circulation model (AGCM) experiments, we demonstrate that this climate change is a response to the temporal history of sea surface temperatures (SSTs). Specifically, 58 of 67 multi-model ensemble members (87%), forced with observed global SSTs since 1950, simulate a positive trend in a winter index of the NAO, and the spatial pattern of the multi-model ensemble mean trend agrees with that observed. An ensemble of AGCM simulations with only tropical SST forcing further suggests that variations in these SSTs are of primary importance. The probability distribution function (PDF) of 50-year NAO index trends from the forced simulations are, moreover, appreciably different from the PDF of a control simulation with no interannual SST variability, although chaotic atmospheric variations are shown to yield substantial 50-year trends. Our results thus advance the view that the observed linear trend in the winter NAO index is a combination of a strong tropically forced signal and an appreciable "noise" component of the same phase. The changes in tropical rainfall of greatest relevance include increased rainfall over the equatorial Indian Ocean, a change that has likely occurred in nature and is physically consistent with the observed, significant warming trend of the underlying sea surface.

J. W. Hurrell (✉) · A. S. Phillips
National Center for Atmospheric Research,
80307-3000 Boulder, CO, USA
E-mail: jhurrell@ucar.edu

M. P. Hoerling · T. Xu
Climate Diagnostic Center, NOAA,
Boulder, CO, USA

1 Introduction

There is ample evidence that most of the atmospheric circulation variability in the form of the North Atlantic Oscillation (NAO) arises from the internal, nonlinear dynamics of the extratropical atmosphere. Interactions between the time-mean flow and synoptic-time scale transient eddies are the central governing dynamical mechanism (Thompson et al. 2003), and these interactions give rise to a fundamental time scale for NAO fluctuations of about ten days (Feldstein 2000). Such intrinsic atmospheric variability exhibits little temporal coherence, so that observed interannual and longer time scale NAO fluctuations could entirely be a statistical remnant of the energetic weekly variability (Wunsch 1999; Stephenson et al. 2000). This *climate noise paradigm* (Leith 1973; Madden 1976), however, fails to explain the enhanced interannual NAO variability observed during boreal winter over the last half of the twentieth century (Feldstein 2000, 2002), including an apparent upward trend in indices of the NAO over this period (Fig. 1).

Thompson et al. (2000) concluded that the observed upward trend of the NAO index in recent decades is statistically significant relative to internal atmospheric variability, and both Gillett et al. (2001) and Feldstein (2002) showed that it is statistically significant compared to red noise models. Furthermore, the observed trend in the winter NAO index is outside the 95% range of internal variability generated in multi-century integrations with seven different coupled climate models (Gillett et al. 2003; Osborn 2004; Osborn et al. 1999; Stephenson and Pavan 2003). This indicates that either the recent NAO behavior is due in part to forcing external to the coupled system, or all of the models are deficient in their ability to simulate North Atlantic interdecadal variability (although the simulated variability is quite similar to that observed in the instrumental record prior to 1950). Comparisons to NAO indices reconstructed from proxy data have also concluded the recent behavior is

Fig. 1 Time series (1950–99) of a January–March index of the NAO from (*top*) observations, (*middle*) the CCM3 GOGA ensemble mean, and (*bottom*) the CCM3 TOGA ensemble mean. The index has units of m and is the difference in 500 hPa heights averaged over a southern (30°N–50°N, 80°W–20°E) minus a northern (60°N–80°N, 80°W–20°W) domain. The time series have been smoothed with a 1-2-1 binomial filter
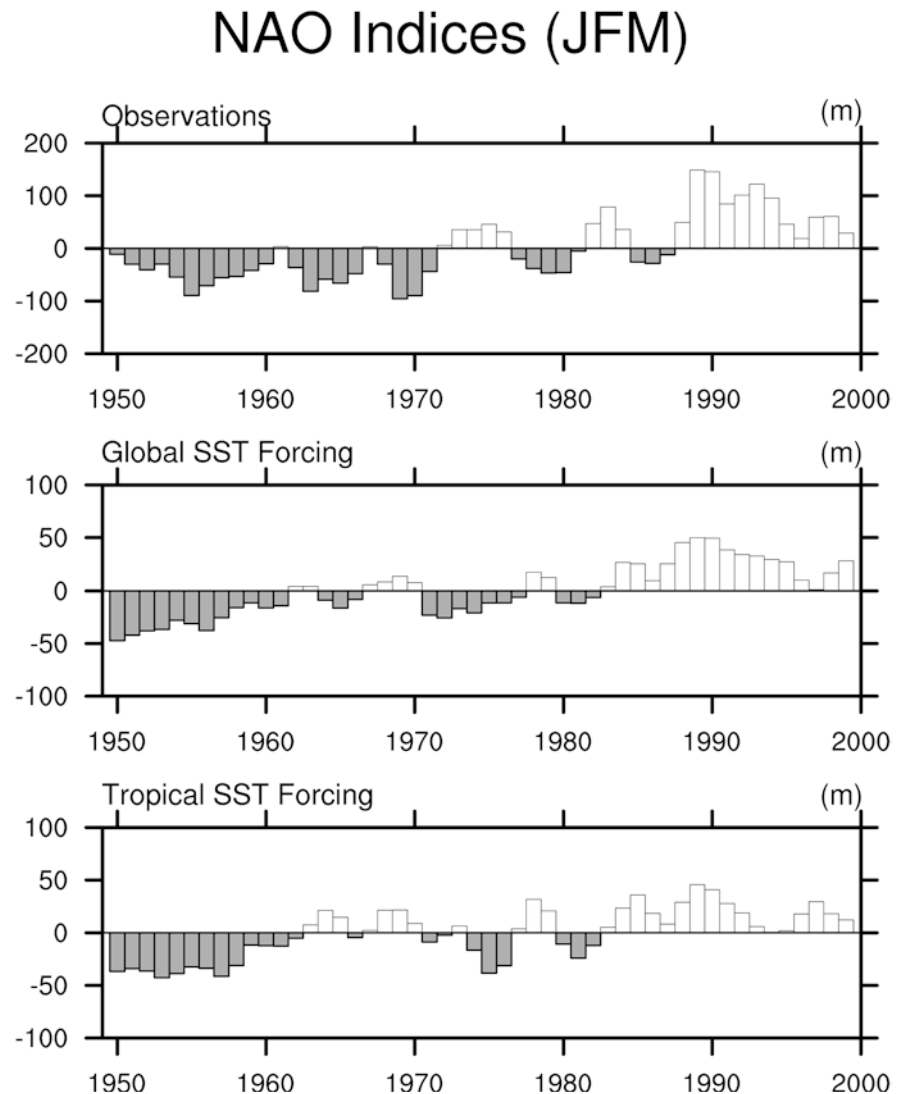
unusual, although perhaps not unprecedented (Jones et al. 2001; Cook 2003). Such extended proxy records, however, are liable to considerable uncertainties (e.g., Schmutz et al. 2000; Cook 2003).

At present, there is no consensus on the process or processes that are most likely responsible for the enhanced interannual variability of the NAO (Hurrell et al. 2003). One proposed source of the recent trend in the observed winter NAO index entails external forcing of the strength of the atmospheric circulation in the lower stratosphere on long time scales by reductions in stratospheric ozone and increases in greenhouse gas (GHG) concentrations (Gillett et al. 2003). The ways by which stratospheric flow anomalies generate further tropospheric variability, however, are not entirely clear. Proposed mechanisms involve the effect of the stratospheric flow on the refraction of planetary waves dispersing upward from the troposphere (Chen and Robinson 1992; Hartmann et al. 2000; Shindell et al. 1999; 2001; Ambaum and Hoskins 2002), columnar adjustment consistent with a "downward control"

principal (Haynes et al. 1991; Black 2002), and zonal-eddy flow feedbacks (Polvani and Kushner 2002).

Another theory is that interactions between the oceans and atmosphere are important for understanding the recent temporal evolution of the NAO (Greatbatch 2000; Marshall et al. 2001; Wanner et al. 2001; Kushnir et al. 2002; Czaja et al. 2003). Using AGCM experiments with prescribed sea surface temperature (SST) anomalies, Robertson et al. (2000) reported substantial increases in simulated NAO variability when observed, interannually varying SSTs were specified over the Atlantic Ocean, relative to a control run forced with climatologically averaged SSTs. Rodwell et al. (1999) and Mehta et al. (2000) further showed that the phase and about 50% of the amplitude of the long-term variability in the wintertime NAO index could be recovered by forcing their AGCMs with the observed time history of global SST and sea-ice distributions over the last half of the twentieth century.

Interpretation of the oceanic role in affecting the phase and amplitude of the NAO hinges critically,

however, on the relative influence of extratropical versus tropical sea surface temperatures. Rodwell et al. (1999), Sutton et al. (2001), and Peng et al. (2003) all demonstrated a NAO-like response to the leading tripole pattern of SST variability over the North Atlantic (Rogers and van Leon 1979; Cayan 1992a,b; Visbeck et al. 2003) implying the time history of NAO variability might be reconstructed from knowledge of North Atlantic SSTs alone. The ambiguity in this interpretation, however, is that the NAO itself is the dominant driver of upper ocean thermal anomalies over the extratropical North Atlantic (e.g., Deser and Timlin 1997; Visbeck et al. 2003), implying minimal North Atlantic climate predictability (Bretherton and Battisti 2000).

Other studies indicate that ocean forcing remote from the extratropical North Atlantic could be important. Sea surface temperature variations in the tropical Atlantic, for instance, occur on a wide range of time scales and involve changes in the meridional SST gradient across the equator (e.g., Marshall et al. 2001). These variations affect the strength and location of tropical Atlantic rainfall that could in turn influence the North Atlantic extratropical circulation (Xie and Tanimoto 1998; Rajagolapan et al. 1998; Venzke et al. 1999; Robertson et al. 2000; Sutton et al. 2001). Hoerling et al. (2001a; hereafter HHX) argued that the most germane analysis of North Atlantic climate variability must consider the role of forcing from the whole tropics, not just the Atlantic sector. In particular, HHX used ensembles of experiments in which an AGCM was forced with the observed temporal evolution of SSTs over only tropical latitudes since 1950 and recovered about half the amplitude of the observed North Atlantic climate change. Moreover, they argued that the tropical Atlantic heating anomalies in their experiments occurred primarily in response to tropic-wide changes in the atmospheric circulation associated with warming surface waters over the tropical Indian and western Pacific Oceans. Sutton and Hodson (2003) also found evidence of tropical Indian Ocean forcing of the NAO on long time scales but, in contrast to HHX, they concluded this effect was likely secondary to forcing from the North Atlantic itself. In contrast, Schneider et al. (2003) concluded the observed trend in the boreal winter NAO index cannot be linked to the warming of the tropical oceans in recent decades; rather, it is more likely a residual of "inter-decadal time scale internal atmospheric noise".

Such divergence of modeling results leaves open the question of oceanic forcing of NAO variability in general, and tropical versus extratropical ocean-atmosphere interactions in particular. In this paper, we expand on the short study of HHX and present new and more comprehensive evidence that the large observed changes in the climate of the extratropical North Atlantic in the form of the NAO since 1950 can indeed be reconciled with forcing by the oceans. We first confirm the robustness of simulated North Atlantic climate trends among ensembles run with four different AGCMs,

where the individual model simulations are forced by specified observed global surface boundary conditions. The models and the experiments are described in detail in the next section. We then further argue, through an ensemble of simulations performed with just one of the AGCMs, that variations in tropical SSTs alone drive much of the North Atlantic change, with changes in rainfall over the tropical Indo-Pacific region being of particular importance. That this result is not model dependent is suggested through an empirical analysis that relates rainfall variations over this region to circulation anomalies over the North Atlantic. It reveals that all four AGCMs exhibit a similar sensitivity to enhanced rainfall over the tropical Indian Ocean. Verification that the models produce realistic changes in rainfall in this region is, therefore, important. We do this through an analysis of available, long station records, as well as through an analysis of the SST and rainfall relationships in fully coupled ocean-atmosphere model simulations. The latter addresses the issue that rainfall variations might be unrealistically constrained by the SST changes in uncoupled AGCM experiments. A new suite of idealized SST anomaly experiments further establishes not only the model independence of our results, but also that the observed North Atlantic circulation changes can be attributed to warming of the tropical Indian Ocean alone. These latter results are presented in a companion paper (Hoerling et al. 2004).

2 Data and methodology

An experiment that has become the standard in the climate research community for evaluating AGCMs and also for determining the ocean forcing of climate variability is that where the models are forced with the known global evolution of (typically) monthly SSTs and sea ice concentrations. Such integrations form the basis of the Atmospheric Model Intercomparison Project (AMIP; Gates et al. 1999), and as such they are commonly referred to as "AMIP" or "Global Ocean Global Atmosphere" (GOGA) experiments. We examine ensembles of GOGA runs performed with four AGCMs (Table 1). Ensemble experiments are carried out in order to detect the climate signal related to the imposed lower boundary forcing, in contrast to individual simulations which, in the extratropics, are dominated by chaotic, nonlinear atmospheric interactions (e.g., Kumar and Hoerling 1995; Mehta et al. 2000). For the moderately sized ensembles examined here, it is important to remember that internal variability might make an important contribution to the variability of the ensemble mean. Although statistical techniques that lead to less biased estimates of the true forced response have been developed (Venzke et al. 1999), we found it insightful to simply examine the statistical behavior within an ensemble by constructing its probability distribution function (PDF). In addition, we examine multi-model ensemble means in order to better estimate the forced

Table 1 The horizontal resolution, number of vertical layers, ensemble size and key references of the AGCMs used in the study

	Horizontal resolution	Vertical layers	Ensemble size	Reference
CCM3	T42	18	12	Kiehl et al. (1998)
ECHAM4.5	T42	18	24	Roeckner et al. (1996)
NSIPP-1	2×2.5, 3×3.75	34	23	Schubert et al. (2002)
ARPEGE	T63	31	8	Cassou and Terray (2001)

climate sensitivity of the real system, as opposed to relying on results from any individual model.

The GOGA ensemble members of a particular model differ from each other only in the specification of the atmospheric initial conditions, which were selected from control integrations of the respective AGCM. All the models employ medium horizontal and vertical resolution with different dynamical formulations and parametrized physics (the reader is referred to the references in Table 1 for further details on the model formulations). In the case of the 23-member NASA Seasonal-to-Interannual Prediction Project (NSIPP-1) model ensemble, nine members were derived using a 2° latitude by 2.5° longitude horizontal resolution, and 14 members were derived using a coarser (3° ×3.75°) resolution. Data from an ensemble of similar size (24 members) were obtained from a recent version of the European Centre-Hamburg model (ECHAM4.5), while a smaller eight-member ensemble was analyzed from a climate model developed jointly by Meteo-France and the European Centre for Medium Range Weather Forecasts (ARPEGE).

We used version 3 of the NCAR Community Climate Model (CCM3; Kiehl et al. 1998) to create not only a 12-member ensemble of GOGA runs, but also an ensemble of equal size to isolate the role of changes in tropical SSTs. In these latter experiments, the time history of observed SSTs was specified over tropical latitudes (30°S–30°N), but CCM3 was forced by a repeating annual cycle of monthly climatological values of SST and sea ice at higher latitudes. These experiments are known as Tropical Ocean Global Atmosphere (TOGA) integrations. A third 12-member ensemble was examined as well, in order to further isolate the influence of the tropical Atlantic Ocean. These runs are documented by Saravanan et al. (2002) and use observed SSTs to force CCM3 over the tropical Atlantic (20°S–20°N), while the atmosphere is coupled to a simple mixed layer ocean model everywhere else. We refer to these as Tropical Atlantic Global Atmosphere (TAGA) experiments.

For the CCM3 and ECHAM4.5 integrations, observed monthly SSTs since 1950 are obtained by merging the empirical orthogonal function (EOF) reconstructed analyses of Smith et al. (1996) through 1981 with the optimal interpolation (OI) SST analyses of Reynolds and Smith (1994) thereafter. The former uses 2° monthly median SST anomaly statistics from the Comprehensive Ocean-Atmosphere Data Set (COADS; Woodruff et al. 1987) and EOF spatial basis functions computed from the more recent OI data, the latter consisting of both *in situ* and bias-corrected satellite-derived SSTs at a finer 1°

spatial resolution. The imposed SSTs for the ARPEGE ensemble come from the United Kingdom Meteorological Office (UKMO) Global Sea-Ice and SST (GISST) dataset of Rayner et al. (1996). Over the period 1949–1981, the GISST SST fields are based on reconstructions using eigenvectors of *in situ* anomalies with a 2° spatial resolution in a fashion similar to that employed by Smith et al. (1996). The analyzed fields from January 1982 onward make use of the Poisson blending technique of Reynolds (1988) to incorporate satellite-derived SST data with *in situ* data from the quality controlled UKMO Historical SST dataset (MOHSST; Bottomley et al. 1990; Parker et al. 1994) and COADS. The nine members of the NSIPP-1 integrations at 2° × 2.5° spatial resolution utilize the GISST analyses prior to 1982 and OI thereafter, while the 14 coarser resolution runs use the UKMO Hadley Centre's sea Ice and SST (HadISST) analyses (Rayner et al. 2003). We analyze the GOGA and CCM3 TOGA integrations over 1950–1999, while the CCM3 TAGA runs are available over 1950–1994. Data from the ARPEGE GOGA experiments are available over 1950–1998.

A brief word is in order regarding the SST forcing data that differ across the various model ensembles. Hurrell and Trenberth (1999) provide a detailed summary of the aforementioned SST datasets (excepting the newer HadISST analysis), as well as a comprehensive comparison among them. They show that some significant differences exist among the monthly SST analyses, largely related to differences in the processing of *in situ* data, and that none is universally the best for all purposes. They demonstrate, moreover, that flaws in the analyzed SST fields can compromise the results of model simulations. The GISST analyses, in particular, have spurious noise and unrealistic temporal persistence of monthly SST anomalies after 1981 (aspects corrected in HadISST; Rayner et al. 2003).

Of more relevance to the current study, however, is the low-frequency behavior of the SST products, including trends. Hurrell and Trenberth (1999) note that global trends in recent years are different between the GISST and OI analyses, and this can be partially traced to differences in the processing of *in situ* data and an increasing cold bias in the OI data arising from incompletely corrected satellite data (improved upon in the updated OI analyses; Reynolds et al. 2002). On multidecadal time scales, the GISST and Smith et al. (1996) SST analyses agree better, likely because the trend is analyzed separately in both products, added back only after the EOF-based reconstruction techniques are

applied. Particularly noteworthy for our purposes, however, is that the best agreement in all statistical measures among the datasets occurs when the SST anomalies are averaged over the tropics. Over this portion of the globe (20°S–20°N), the large interannual variability associated with the El Niño/Southern Oscillation (ENSO) phenomenon is well captured in each SST analysis, and all products show a similar warming trend since 1950, although the warming is slightly less over the last two decades in the OI analysis.

3 Results

3.1 Revisiting the CCM3 results of HHX

Evidence for the viewpoint that North Atlantic climate variability is not merely stochastic atmospheric noise, but rather contains a response component to changes in ocean surface temperatures and/or sea ice, comes from a comparison of observed and CCM3-simulated NAO indices for the boreal winter season of January through March (JFM; Fig. 1). The indices are based on the difference of 500 hPa heights averaged over a southern (30°–50°N, 80°W–20°E) minus a northern (60°–80°N, 80°W–20°W) domain, and they have been temporally smoothed with a simple 1–2–1 binomial filter. The regions are near the NAO centers-of-action as indicated from a regional EOF analysis of JFM 500 hPa height anomalies (not shown). The data source for observed 500 hPa heights is the NCEP/NCAR reanalysis (Kalnay et al. 1996).

It is clear that the low-frequency behavior in the simulated NAO time series from global SST forcing, including an overall upward trend, closely resembles that observed, although the amplitude of the GOGA ensemble mean is about one-half of that observed. The unsmoothed (smoothed) GOGA and observed NAO time series are correlated at 0.37 (0.61), which is significant at the 5% level. HHX showed a similar result (correlation of 0.8), but from a more heavily filtered NAO index based on monthly data through the year. The linear trend of the GOGA time series is 70 ± 14 m, relative to an observed value of 149 ± 42 m, where the 95% confidence intervals were estimated accounting for the correlation in the monthly residuals from the linear trend fit. These results confirm the conclusions of Rodwell et al. (1999) and Mehta et al. (2000) that slow changes in the state of the world oceans force the North Atlantic atmosphere on longer time scales.

But what portion or portions of the world oceans are most critical? HHX regressed the boreal winter global SST field onto their low-pass filtered NAO index and found, both in the CCM3 and observations, a coherent pattern of tropic-wide warm SSTs associated with the positive index phase of the NAO (their Fig. 2). This motivated their examination of the 12-member CCM3 TOGA ensemble, although they did not present the ensemble mean NAO index from those integrations. It is

shown in the lower panel of Fig. 1, and it is clear that the time evolution of the NAO in the GOGA simulation is largely reproduced as a result of tropical SST forcing alone: the correlation between the two unsmoothed (smoothed) ensemble-mean time series is 0.64 (0.83), and the linear trend of the ensemble-mean TOGA NAO index is 65 ± 15 m.

The time series in Fig. 1 also confirm a linear trend to be a reasonable description of the low-frequency change in North Atlantic climate since 1950. The spatial details of the observed and simulated trends in 500 hPa height are depicted in Fig. 2, where the AGCM ensemble-mean trends have been multiplied by a factor of two. Here our focus is strictly on the North Atlantic sector, which can be compared to hemispheric (20°–90°N) maps in both HHX and our companion paper.

Both the GOGA and TOGA ensembles capture the trend toward lower heights over the subpolar North Atlantic and higher heights over middle latitudes, although some regional details differ from observations. For both ensemble mean patterns, the spatial correlation
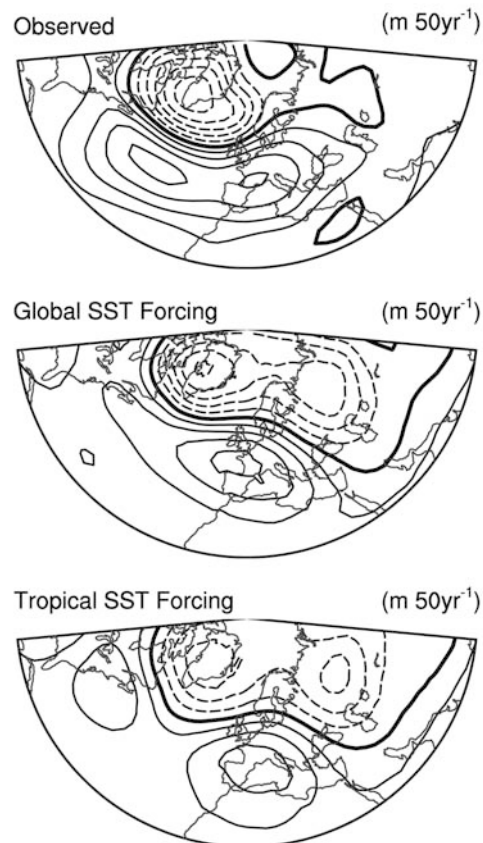
Fig. 2 The linear trend (1950–99) of January–March 500 hPa heights from (*top*) observations, (*middle*) the NCAR CCM3 GOGA ensemble mean, and (*bottom*) the CCM3 TOGA ensemble mean. The model trends have been multiplied by a factor of two. The contour increment is 20 m per 50 years, negative trends are *dashed*, and the zero contour is given by the *thick black line*

with the observed trend map is near 0.7 over the domain shown. That tropical SST forcing alone captures the main features of the change argues that extratropical SSTs are not generating a strong feedback in the GOGA integrations (see also Peterson et al. 2002; Lin et al. 2002; Lu et al. 2004; Schneider et al. 2003).

3.2 Reproducibility

Before the tropical forcing issue is pursued further, it is important to establish the reproducibility of the simulated North Atlantic trend. In particular, how model dependent are the results, how reproducible is the North Atlantic climate change signal among individual ensemble members, and what, if any, aspects of the change are deterministic in the SST forcing?

The patterns of local height trends simulated in the ECHAM4.5, ARPEGE and NSIPP-1 GOGA ensembles are very to similar to the CCM3 pattern, and all project strongly onto the positive index phase of the NAO (Fig. 3). The spatial pattern and amplitude of change is most consistent between NSIPP-1 and CCM3, where local trends on the order of 30 m over 50 years are evident. The ARPEGE ensemble simulates changes of similar amplitude, although the entire pattern is shifted slightly to the south relative to CCM3 and NSIPP-1. The weakest trends are evident in the ECHAM4.5 ensemble.

To further evaluate the reproducibility of the North Atlantic climate change, we computed the linear trend (1950–1999) of the NAO index (defined as in Fig.1) for each of the 67 multi-model GOGA integrations and plotted the estimated PDF of these trends (Fig.4). The mode (median) of the multi-model distribution has a value of 50 m (44 m), and noteworthy is that 58 of the 67 GOGA members (87%) simulate a positive NAO index trend. This sample thus indicates that the phase of the NAO change since 1950 was virtually determined by the temporal history of global SSTs. The PDFs constructed from the ensemble members of each model separately (not shown) are consistent with the multi-model PDF and with the magnitude of the ensemble mean trends of each AGCM seen in Fig. 3. Thus, while 21 of the 24 ECHAM4.5 integrations yield a positive NAO index trend, the median is only 26 m, while the medians of the other three AGCM distributions are near or exceed 50 m. Although the sample size is much smaller (12 members), the estimated PDF of the CCM3 TOGA ensemble is plotted as well. Its distribution has a mode (median) of 60 (54) m and is very similar to the multi-model GOGA distribution.

Further evidence that SST forcing in general, and tropical SST forcing in particular, is responsible for the upward trend in the simulated NAO indices since 1950 is provided by the PDF computed from a long control simulation with CCM3. In this integration, only climatological annual cycles of SST and sea ice were

Linear Trend 500hPa Z (JFM) 1950-99
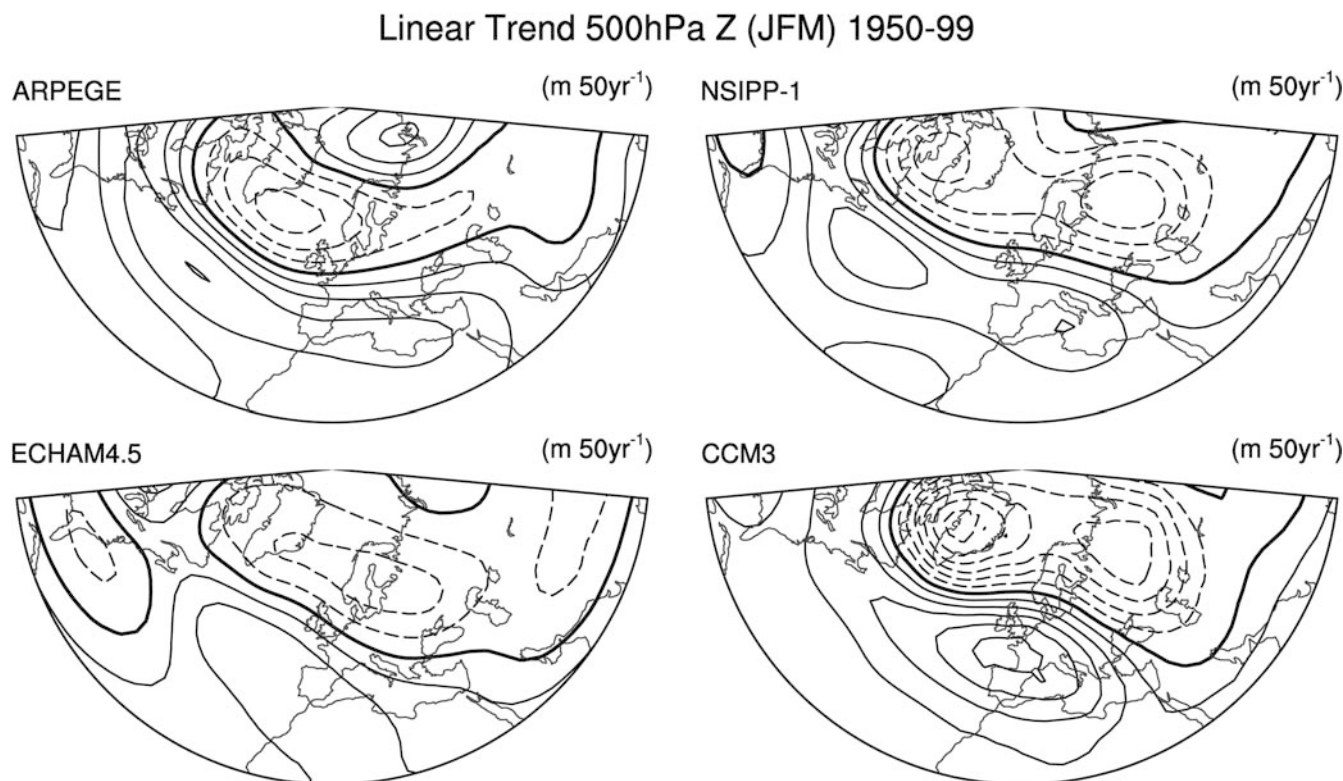
Fig. 3 The linear trend (1950–99) of January–March 500 hPa ensemble mean heights from GOGA simulations with four different AGCMs, as described in the text. The contour increment is 8 m per 50 years, negative trends are *dashed*, and the zero contour is given by the *thick black line*

Fig. 4 Estimated probability distribution functions (PDFs) of the January–March linear trend (1950–99) of an NAO index (defined as in Fig. 1) for: a 67-member ensemble of GOGA simulations across four AGCMs (*solid*), a 12-member ensemble of TOGA simulations with the NCAR CCM3 (*dashed*), and a long control integration with the CCM3 forced by climatological annual cycles of SST and sea ice (*dotted*). The observed linear trend (149 ± 42 m) is given by the *solid, vertical bar*


Trend of JFM 500hPa NAO index (1950-99)
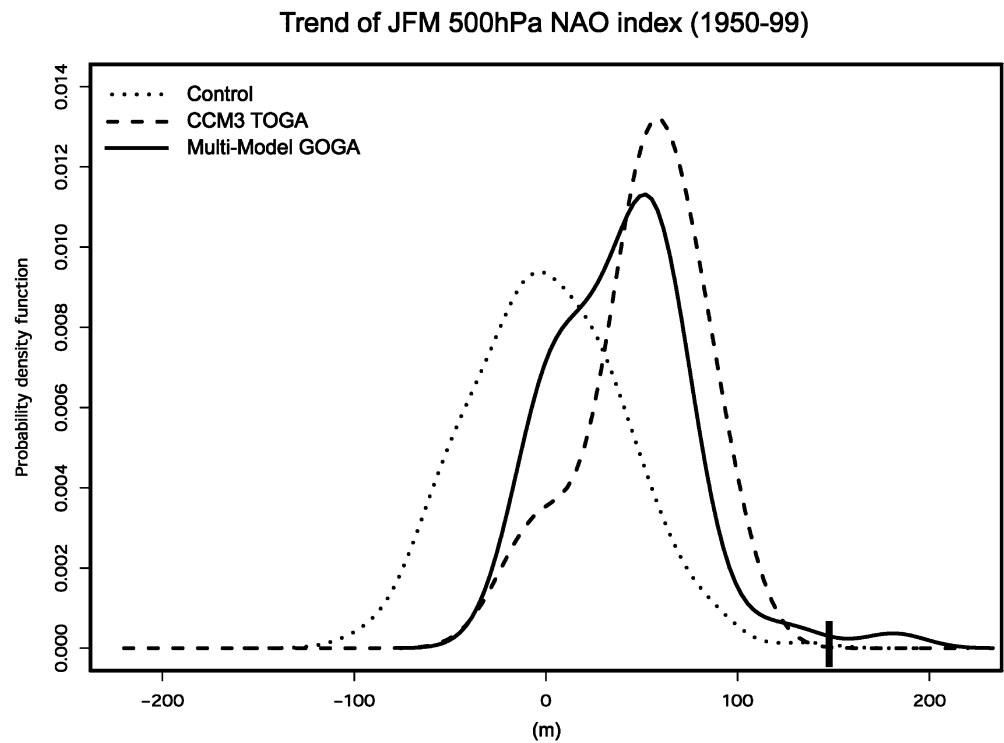
specified, so the distribution represents the NAO index trend values resulting from internal atmospheric dynamical processes alone. A sample size of 100 independent 50 year trends was obtained by Monte Carlo sampling, a strategy justified by the fact that the year-one lag autocorrelation of the index from the 199 year control run was near zero (–0.03). Consistent with the notion of a stochastic process, the distribution of this PDF is significantly different from the boundary-forced GOGA and TOGA distributions, with a mode near zero and a standard deviation of 39 m. In other words, the mode of the TOGA PDF is positively shifted by ∽ 1.5 standardized departures of the 50 year NAO index trend values that arise solely from processes intrinsic to the atmosphere, although it is also clear that chaotic atmospheric variations alone yield appreciable 50 year trends (e.g., Schneider et al. 2003).

Relative to the observed linear trend of 149 ± 42 m, the simulated NAO index trends are of smaller amplitude, generally by a factor of two to three. This underestimation could be due to a number of factors. It is conceivable, for instance, that the mode of the multi-model PDF represents the true forced signal, and that the observed trend includes this plus a random component. Two of the individual realizations, after all, have NAO index trends that exceed the observed magnitude. On the other hand, the underestimation could reflect deficiencies in the models or the experimental design. Examples of the former include unrealistically low sensitivity to SST variations, or missing feedbacks, for instance related to coarse vertical reso-

lution and an inability to capture the mechanisms by which stratospheric anomalies may affect the evolution of the troposphere (e.g., Shindell et al. 2001; Zhou et al. 2001). Possible deficiencies in the experimental design include the fact that AMIP integrations are one-way forcing experiments, so that the damping effect on surface fluxes associated with the finite heat capacity of an interactive ocean is missing (e.g., Barsugli and Battisti 1998), or that important changes in other external forcings since 1950 (e.g., changes in ozone or greenhouse gas concentrations) have not been considered. Even with these possible limitations, the results strongly argue that SST changes have had an important controlling effect on North Atlantic climate change since 1950.

The spatial pattern of the multi-model ensemble mean 500 hPa height trend, as well as the trend in simulated total precipitation over the North Atlantic domain, is shown in Fig. 5. The spatial pattern of the height change agrees well with the observed (Fig. 2a): the spatial correlation between the two is 0.75, higher than for any individual model ensemble average. The main difference is that the models simulate large wintertime height falls over Scandinavia and northern Russia that have not been observed. The precipitation trend is toward drier conditions across the entire Mediterranean region into Southwest Asia, with wet trends covering northern and eastern Europe and most of Scandinavia. Consistent with the reproducibility of the NAO index trends (Fig. 4), these regional precipitation trends are also highly reproducible among the 67 GOGA realizations (not shown).

Linear Trend (JFM) Multi-AGCM 1950-99
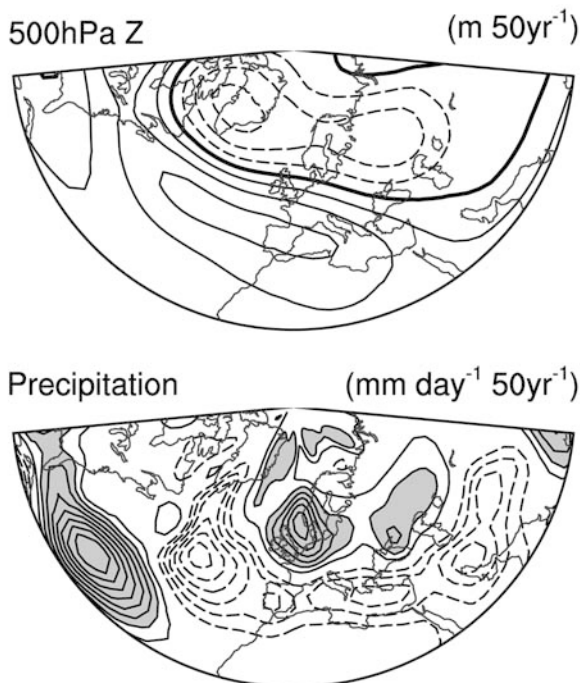
Fig. 5 The linear trend (1950–99) of the January–March multi-model ensemble mean (*top*) 500 hPa heights and (*bottom*) total precipitation. The ensemble means were computed from 67 individual GOGA simulations across four different AGCMs. The contour increment for the height trend is 8 m per 50 years, negative trends are *dashed*, and the zero contour is given by the *thick black line*. The contour increment is 0.05 mm day^{-1} per 50 years for the precipitation trend, the zero contour is omitted, and regions with a trend exceeding +0.1 mm day^{-1} per 50 years are *shaded*

Because of the paucity of long-term rainfall records over the oceans, the trend in precipitation over the North Atlantic Ocean cannot be verified. The simulated long-term changes, however, are consistent with the known pattern of interannual rainfall variability associated with the NAO. As shown by Hurrell (1995) among others, positive NAO index winters are typified by drier-than-average conditions over the middle latitudes of the North Atlantic Ocean into southern Europe, the Mediterranean and parts of the Middle East, while dry conditions also prevail over the Labrador Sea. In contrast, positive NAO index winters produce anomalously high precipitation rates from Iceland through Scandinavia. Hurrell and van Loon (1997) analyzed station data over 1981–1994 and showed, furthermore, that the 14 winter average precipitation anomalies (relative to the 1951–1980 mean) were of the same sense as the aforementioned pattern of interannual variability over Europe. Thus, we conclude the multi-model simulated trend in boreal winter precipitation over the North Atlantic sector likely has many aspects in common with observed changes since 1950, and that the evolving global SSTs have exerted an important controlling effect on the phase of this pattern.

3.3 Changes in tropical SST and rainfall

The analysis of HHX implied the existence of a link between the low frequency variability of North Atlantic climate since 1950 and an anomalously warm pattern of the tropical oceans that resembles the tropical SST trend itself. In Part II of this study, we present the scientific evidence for a causal link between these two trend components. Here, we first analyze the structure of the SST trend and its relation to changes in tropical rainfall.
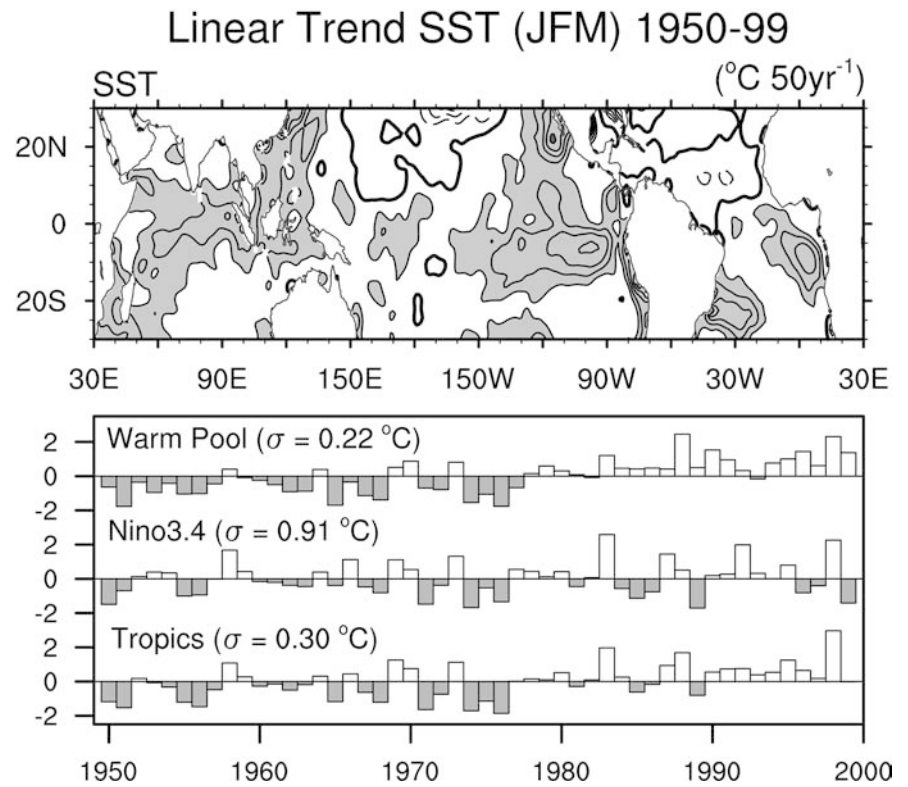
The linear trend in JFM SST over the tropical oceans since 1950 estimated from HadISST (Fig. 6) reveals widespread warming, most notably over the tropical Eastern Hemisphere with rates greater than 1°C per 50 years over portions of the Indian and western Pacific Oceans. The rate of warming has also been large over the South Atlantic Ocean and off the Equator in both hemispheres over the eastern Pacific Ocean. There are also notable regional cooling trends over the subtropical North Pacific and tropical North Atlantic Oceans. The cooling in the latter region is consistent with enhanced northeasterly trade winds associated with the trend toward the positive index phase of the NAO over this period (Visbeck et al. 2003).

Which, if any, of the tropical SST changes are, in fact, meaningfully characterized as linear trends? In the lower panels of Fig. 6 are shown several SST time series, presented as standardized departures from the 1950–1999 mean. For the tropics (15°S–15°N) as a whole, the rate of warming during JFM has been 0.46 ± 0.25°C per 50 years. The relatively large error bars on the trend estimate reflect statistical uncertainty associated with large interannual variations that are dominated by ENSO, as evidenced by the similarity (linear correlation of 0.83) between the tropical and Niño3.4 (170°W–120°W; 5°S–5°N) SST time series. Moreover, over the central and eastern equatorial Pacific, observed changes in SST cannot be adequately described by a linear fit: they involve, for instance, increases in the interannual variability over the last few decades. In contrast is the warming over the Indian and western Pacific Oceans. In this "warm pool" region (60°E–170°E; 15°S–15°N), the rate of warming since 1950 is highly significant (0.62 ± 0.13°C) and is well described by a linear trend.
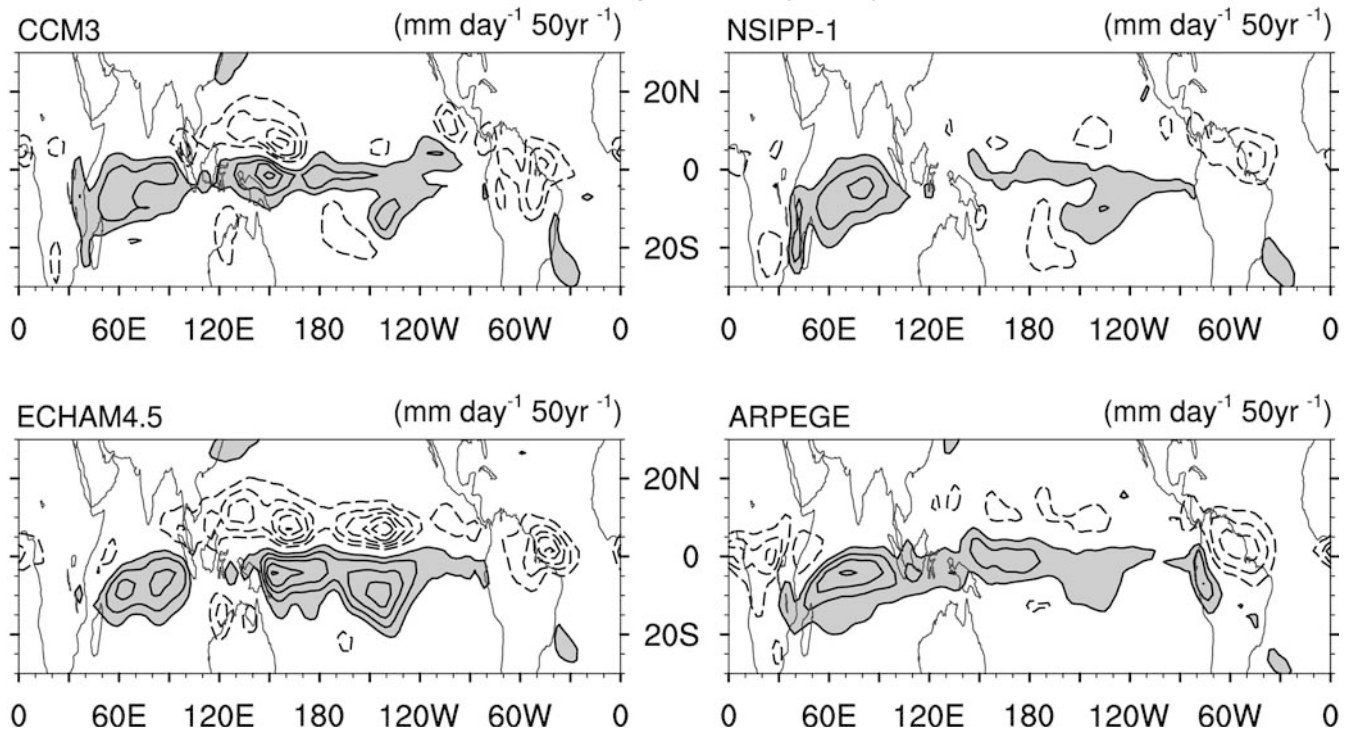
The physical link by which North Atlantic climate would respond to tropical forcing involves changes in diabatic heating anomalies associated with changes in rainfall. Presented in Fig. 7 is the linear trend in JFM precipitation since 1950 as simulated by the four AGCMs. For CCM3, we have combined the TOGA and GOGA integrations to produce a 24-member ensemble. All the models simulate increased precipitation over the equatorial Indian Ocean that extends eastward toward the central Pacific, a response that is physically consistent with the warming trend of the underlying sea surface. On the poleward flanks of this increase, a drying trend is simulated, and decreases in rainfall are evident from equatorial South America across the Atlantic Ocean into Africa as well. Overall, the patterns have

Fig. 6 (*Top*) The linear trend (1950–99) of January–March (JFM) observed tropical SST with a contour increment of 0.25 °C per 50 years (starting at ± 0.50 °C). Positive (negative) trends are *shaded* (*dashed*). (*Bottom*) time series of normalized JFM SST anomalies over the Indian and western Pacific Ocean "warm pool" (60°E–170°E, 15°S–15°), the central equatorial Pacific "Niño3.4" region (170°W–120°W, 5°S–5°N), and the entire tropics (15°S–15°N). The standard deviations (°C) of each series are indicated
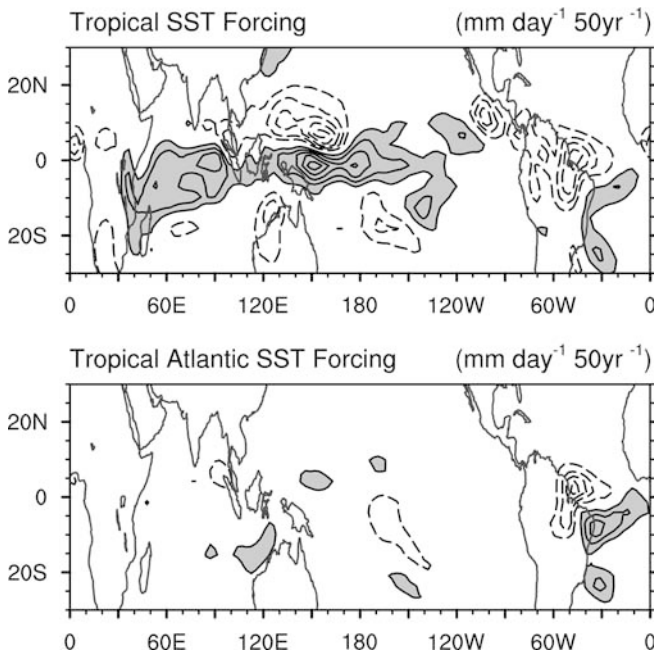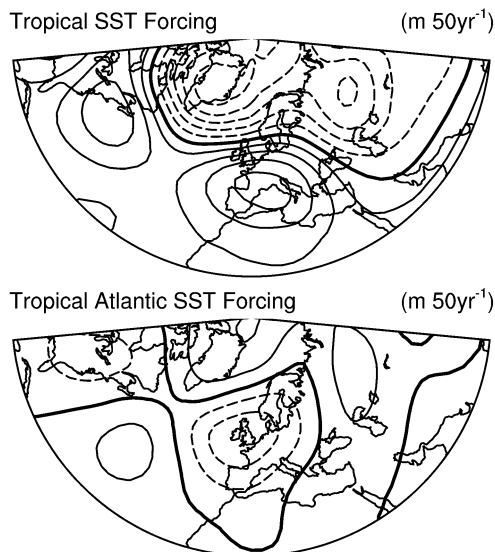

Fig. 7 The linear trends (1950–99) of January–March tropical precipitation simulated by four different AGCMs forced with the observed temporal evolution of tropical SSTs. The contour increment is 1.0 mm day^{-1} per 50 years, the zero contour is omitted, and positive (negative) trends are *shaded* (*dashed*)

Linear Trend Precipitation (JFM) 1950-94

Fig. 8 The linear trend (1950–94) of January–March tropical precipitation simulated by the NCAR CCM3 from the (*top*) TOGA ensemble mean and (*bottom*) TAGA ensemble mean. The contour increment is 1.0 mm day^{-1} per 50 years, the zero contour is omitted, and positive (negative) trends are *shaded* (*dashed*)

Linear Trend Z500 (JFM) 1950-94

Fig. 9 The linear trend (1950–94) of January–March 500 hPa height simulated by the NCAR CCM3 from the (*top*) TOGA ensemble mean and (*bottom*) TAGA ensemble mean. The contour increment is 8 m per 50 years, negative trends are *dashed*, and the zero contour is given by the *thick black line*

some features in common with the interannual rainfall signal associated with ENSO, but the large zonal scale of enhanced rainfall and the strong response over the

Indian and western Pacific Oceans are different. The general agreement among the AGCMs argues that the results are not unduly sensitive to the representation of moist processes such as clouds and convection in the models employed. The most noticeable difference is the strong, banded rainfall response over the western and central Pacific in ECHAM4.5.

Which changes in tropical rainfall are most important in driving the North Atlantic climate change? While this issue is explored in depth in the companion study, we note here that the appreciable drying over the equatorial Atlantic and South America is of particular interest based on existing evidence in the literature. In particular, it has been suggested in other AGCM studies that variations in tropical and subtropical Atlantic SSTs affect convective activity that in turn produces a remote response over the North Atlantic (Venzke et al. 1999; Robertson et al. 2000; Sutton et al. 2001) akin to the atmospheric bridge mechanism operating over the Pacific during ENSO (Alexander et al. 1992; Trenberth et al. 1998). There is also some observational evidence of a statistical link between the NAO and tropical and subtropical Atlantic SSTs (Xie and Tanimoto 1998; Rajagolapan et al. 1998).

To explore the role of the tropical Atlantic in producing the observed low-frequency climate variations over the North Atlantic, we present the linear trend in JFM rainfall from the 12-member TAGA ensemble mean (Fig. 8). Tropical Atlantic SST variations reproduce the local trends in rainfall evident in the Atlantic sector in the TOGA ensemble (upper panel) quite well, in contrast to the independent five-member ensemble mean TAGA experiments examined in HHX. Consistent with their results, however, rainfall trends outside of the tropical Atlantic are small, and the changes in tropical Atlantic rainfall do not appear to be the primary driver of the NAO-like pattern of height change over the extratropical North Atlantic. Evidence for this is revealed by the linear trend in JFM 500 hPa heights over the North Atlantic from both the CCM3 TOGA and TAGA ensembles (Fig. 9). The pattern of change recovered from tropical Atlantic SST forcing alone does not resemble that captured from full tropical SST forcing, and the simulated TAGA NAO time series (not shown) exhibits no correlation with the observed (Fig.1). We thus conclude that North Atlantic climate change in the form of the NAO index trend since 1950 likely originates from tropical forcing outside of the Atlantic basin.

It therefore becomes important to document several further characteristics of tropical forcing over the Indian and Pacific Ocean basins, and especially their different temporal behaviors since 1950. A comparison of JFM seasonal precipitation time series from the 79-member multi-model ensemble mean is shown in Fig. 10 for the warm pool and Niño3.4 regions. The simulated variations in both regions appear to be strongly constrained by the evolution of the underlying sea temperatures (Fig. 6). Over the central and eastern

Fig. 10 Time series (1950–99) of normalized January–March multi-model ensemble mean precipitation anomalies over (*top*) the Indian and western Pacific Ocean "warm pool" (60°E–170°E, 15°S–15°) and (*bottom*) the central equatorial Pacific "Niño3.4" region (170°W–120°W, 5°S–5°N). The standard deviations (mm day^{-1}) of each series are indicated, and the ensemble mean data were computed from 79 individual GOGA and TOGA simulations across four different AGCMs
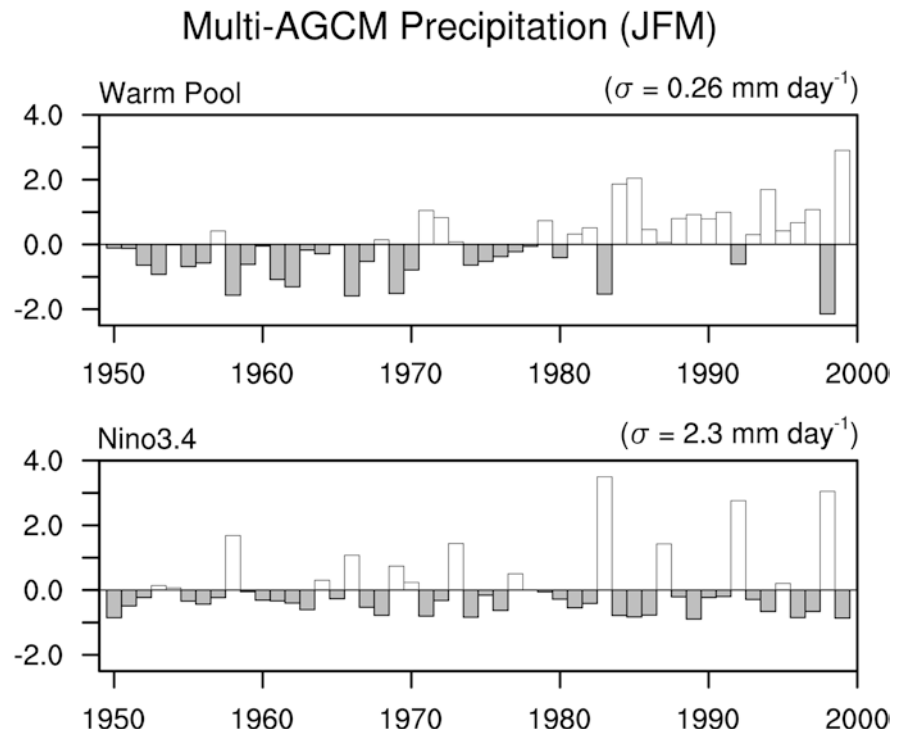
Pacific, large rainfall anomalies occur on interannual time scales in response to ENSO events: the linear correlation between the observed JFM Niño3.4 SST and simulated precipitation is 0.89 over 1950–1999. In contrast, the interannual fluctuations of warm pool precipitation are only modestly correlated (0.23) with interannual fluctuations of warm pool SSTs. During El Niño events, for example, warm pool rainfall is depressed by large-scale subsidence even though local SSTs are warm (e.g., Trenberth and Caron 2000). This observed relationship is evident in the model data as well: the correlation between simulated warm pool and Niño3.4 rainfall anomalies (Fig. 10) is –0.57, while the correlation between observed JFM SST anomalies in the two regions (Fig. 6) is 0.47. On longer time scales, however, the simulated warm pool rainfall exhibits a clear positive trend (Fig.10), which is physically consistent with the highly significant warming trend in Indian and western Pacific Ocean SSTs (Fig. 6).

### 3.4 Sensitivity to Indian Ocean rainfall

There are few indications for a NAO-like response to rainfall variations over the central and eastern Pacific. Most evidence, for instance, suggests the impact of ENSO on the NAO is small, and any link that might exist appears to be most likely when conditions are cold in the equatorial Pacific (e.g., Pozo-Vázquez et al. 2001; Cassou and Terray 2001). Conversely, there are indications from several case studies of a North Atlantic seasonal response to the unusually warm Indian Ocean waters observed in recent winters, and this response projects strongly onto the positive index phase of the NAO (Ferrara et al. 2000; Hoerling et al. 2001b; Pegion et al. 2001). In addition, Miller et al. (2003) document a statistically significant relationship over 1979–2001 between observed monthly increases in convection over the tropical Indian Ocean and the positive index phase of the NAO (see also Weickmann et al. 1985).

To assess the potential role of long-term changes in Indian Ocean rainfall in driving the boreal winter height trend pattern over the North Atlantic (Fig. 3), we constructed a multiple linear regression model to identify the intrinsic extratropical atmospheric anomalies associated with tropical (20°S–20°N) rainfall anomalies. The analysis was performed for each of the four AGCMs separately in order to assess model dependency. First, the monthly (December, January, February and March) precipitation and 500 hPa height data from the GOGA simulations were concatenated to form long time series (e.g., 23 integrations × 50 year × 4 months = 4600 months from the NSIPP–1 ensemble). Next, the tropical monthly rainfall anomalies were projected onto a 50-member EOF basis, which for each model retained over 90% of the monthly rainfall variance, and then a weighted average of the rainfall EOFs was formed to construct a desired empirical rainfall anomaly pattern. The atmospheric circulation associated with this rainfall anomaly was derived by regressing 500 hPa heights onto the principal component time series of each rainfall EOF, then finally summing across all regressions.

The results of a calculation in which the targeted empirical rainfall anomaly is an increase in precipitation

Empirical Sensitivity 500hPa Z (DJFM)
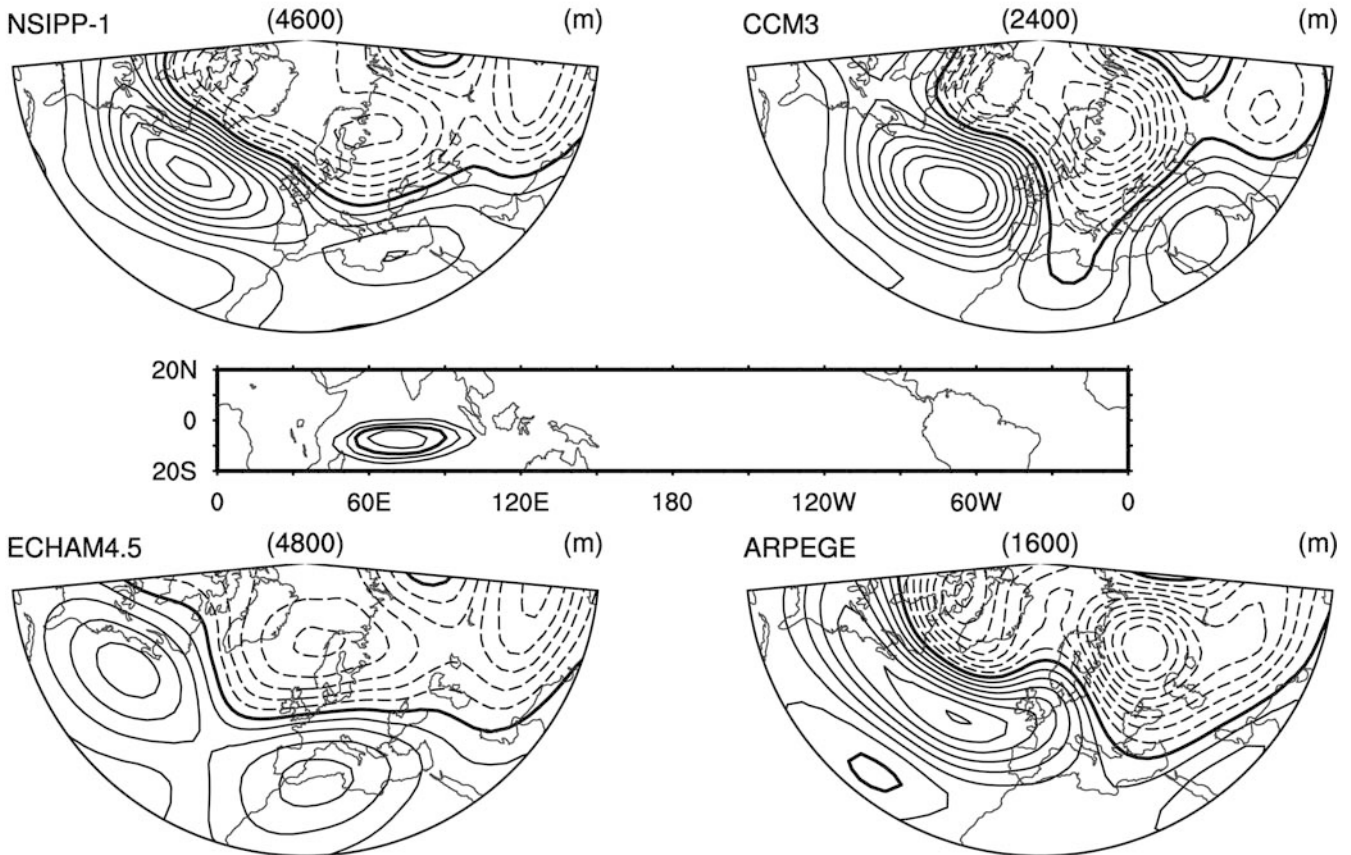
Fig. 11 Multiple linear regression patterns for four AGCMs of the winter 500 hPa height anomalies associated with a +10 mm day⁻¹ monthly averaged rainfall anomaly over the Indian Ocean centered at 70°E, 7°S (see text for details). The number of winter (December–March) months used in the calculation is indicated in *parentheses*. The contour increment is 5 m, negative contours are *dashed* and the zero contour is indicated by the *thick black line*. The average tropical precipitation response across the four models is shown in the *middle panel* with a contour increment of 2 mm day⁻¹

of 10 mm day⁻¹ at 7°S, 70°E is shown in Fig. 11. The empirically-derived precipitation anomaly is presented in the middle panel. It reveals an increase in rainfall spanning the Indian Ocean south of the Equator with maximum amplitude from roughly 50°–100°E, corresponding closely to the pattern of Indian Ocean rainfall trend seen in the GOGA simulations (Fig. 7). The monthly North Atlantic 500 hPa patterns that go along with the enhanced Indian Ocean rainfall are similar among the four models, and in each case project onto the positive index phase of the NAO. The empirically derived sensitivity patterns furthermore strongly resemble the GOGA linear trend patterns of Fig. 3. The spatial correlation with the GOGA trend pattern for NSIPP–1 is 0.90, while it is 0.77 for both CCM3 and ECHAM4.5 but only 0.39 for the southward shifted trend pattern of GOGA ARPEGE. Very similar results are obtained when the targeted rainfall anomaly is moved to other longitudes within the Indian Ocean basin (not shown).

It is important to note that such a statistical analysis is ambiguous with respect to cause and effect. It only

reveals that enhanced Indian Ocean rainfall in each of the AGCM GOGA ensembles is linearly associated with circulation anomalies over the North Atlantic that resemble the positive index phase of the NAO, similar to the relationship documented in observations by Miller et al. (2003). It suggests, however, that the simulated positive trends in Indian Ocean rainfall could be an important driver of North Atlantic climate change. It is therefore important to verify the GOGA models are producing realistic, long-term changes in rainfall in this region.

3.5 Observed changes in warm pool rainfall

Limitations in observational data throughout the tropics do not permit a definitive verification of the simulated 1950–1999 rainfall trends (Fig. 7). Tropical rainfall variations in the NCEP/NCAR reanalysis should be viewed as another "model" estimate, although we note the linear trends in JFM rainfall from those assimilated data (not shown) look much like the GOGA trends

analyzed here. Observational records from tropical stations are usually short and incomplete in time, and changes in instrumentation and other factors often make trend estimates unreliable. Nevertheless, we have analyzed records of tropical rainfall from stations through the Indo-Pacific region, and the 1950–1999 linear rainfall trends for four of those stations are presented in Fig. 12. The stations were selected based on the relative completeness of their rainfall records over the January through March months since 1950. The data source is version 2 of the Global Historical Climatology Network (Vose et al. 1992). No attempt has been made to correct for possible inhomogeneities in the records, however, and the station-based trend values should thus be viewed with considerable caution. In each record, interannual variability is large and only the JFM rainfall trend at Colombo, Sri Lanka (6.9°N, 79.9°E) was significantly different from zero at the 5% level. All numerical values in the following discussion have units of mm day^{-1} 50 year^{-1}.

For comparison to the station data, the distributions of the linear trends in rainfall from the 79 individual multi-model ensemble members are also plotted. Model data were area-averaged over immediate grid boxes closest to the station locations. In each case, the simulated rainfall changes are consistent with the 1950–1999 JFM rainfall trends estimated from the available station records (Fig. 12). Near Diego-Suarez, Madagascar (12.3°S, 49.3°E) and Agalega, Seychelle Islands (10.6°S, 56.8°E), all individual ensemble members simulate positive rainfall trends. The trend distributions at these stations are characterized by median (standard deviation) values of 1.5 (0.9) and 2.7(1.1), respectively, in comparison to observed rainfall trends of 2.1 ± 3.1 (Diego-Suarez) and 0.5 ± 1.7 (Agalega). Rainfall anomalies at the latter station were missing or negative in recent years: the 1950–1994 trend value in comparison was 1.8 ± 1.9.

The models also capture observed drying trends over the northern Indian Ocean. At Colombo, the trend in observed rainfall (–1.9 ± 1.3) agrees in sign but is larger in magnitude than the median of the simulated distribution (–0.7), which has a standard deviation of 0.8. Near Kuantan, Malaysia (3.8°N, 103.2°E) most members of the multi-model distribution simulate a drying trend (median of –1.7, standard deviation of 0.9), as is observed –2.6 ± 3.7.

Long-term rainfall records at stations throughout the Philippines and Indonesia were examined as well. Most of them were incomplete, and it was not possible to

Fig. 12 (*Top*) the linear trend (1950–99) of the January–March (JFM) multi-model ensemble mean total precipitation over the tropical Indian and western Pacific Oceans. The contour increment is 0.5 mm day^{-1} per 50 years, the zero contour is omitted, and positive (negative) trends are *shaded* (*dashed*). The ensemble mean was computed from 79 individual GOGA and TOGA simulations across four different AGCMs. (*Bottom*) the estimated PDFs of the simulated JFM rainfall trends at four stations, indicated by the *letters A-D*, from the 79-member ensemble. The observed linear trends at each station are given by the *vertical bars*, and the units are mm day^{-1} per 50 years
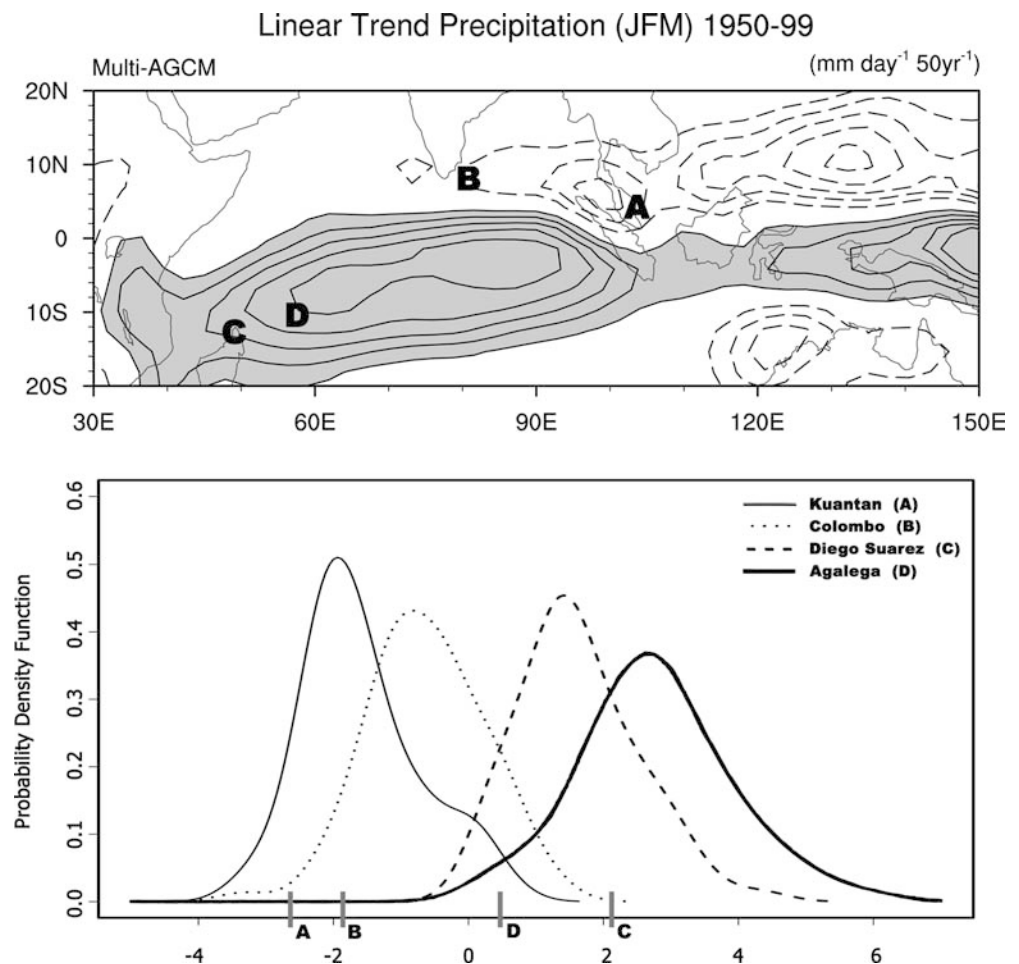
reliably compute the observed long-term change in JFM rainfall since 1950. For those that had more complete records, however, general agreement with the simulated trends was found. For instance, near Aparri, Philippines (18.4°N, 121.6°E), the observed trend is only –0.7 ± 1.4, while the median of the simulated distribution is near zero (–0.1) and the spread among individual members is small (σ = 0.4). Moreover, the GOGA rainfall trends over the western Pacific qualitatively agree with the observational analyses of Deser et al. (2004), who examine epoch differences in tropical precipitation associated with interdecadal variations in North Pacific climate. The one notable exception is over northwestern Australia, where the observed trend in JFM rainfall since 1950 has been toward wetter conditions (not shown). Overall, however, it is reasonable to claim that the simulated changes in rainfall over the warm pool region are consistent, at least in sign, with estimates of observed JFM rainfall trends.

It is also interesting to note that experiments with coupled ocean-atmosphere models simulate increases in Indian Ocean SST and rainfall similar to those observed and simulated by the GOGA integrations. We examined a historical (1870–1998) integration performed with a version of the NCAR Climate System Model (CSM; Boville and Gent 1998) forced with estimated time-dependent changes in sulfate aerosol and greenhouse gas concentrations. The linear trend (1950–1998) of the simulated JFM warm pool SST time series was 0.59 ± 0.14 °C, in good agreement with the observed rate of warming over this region (Fig. 13). The model also simulated a long-term increase in rainfall from 15°S to the Equator across the Indian Ocean into the central Pacific (not shown), although with more pronounced drying on the poleward flanks than simulated by the GOGA integrations (Fig. 12). The maximum amplitude of the JFM rainfall increase over the equatorial Indian Ocean in the fully coupled simulation, however, agrees well with that of the prescribed ocean experiments, and similar rainfall changes were evident in a three-member ensemble of historical simulations with a coupled ver-

sion of the ECHAM model (not shown). From such comparisons, we conclude that the amplitude of the tropical Indo-Pacific rainfall trends in the GOGA simulations is not overly constrained by the lack of an interactive ocean.

4 Conclusion

4.1 Summary

Time series of atmospheric, oceanic, and ecological indices describing North Atlantic climate variability have been tantalizing in their suggestion of unusual, if not unprecedented, change since 1950 (Hurrell et al. 2003). We have presented evidence that slow SST variations have had an important controlling effect on North Atlantic climate over this period, with a warming trend of tropical Indian and western Pacific Ocean surface temperatures being of particular importance. This possibility was first argued for by HHX, but we have expanded on that short study in several significant ways.

First, we have shown that the North Atlantic climate trends, resembling the positive polarity of the NAO, are consistently reproduced among four AGCMs forced with the observed evolution of global SSTs since 1950. Independent studies using two versions of the Hadley Centre model found similar results as well (Rodwell et al. 1999; Sutton and Hodson 2003), although one other study using another AGCM did not (Schneider et al. 2003). To minimize the impact of individual model errors, multi-model ensemble means and their associated PDFs were examined. The spatial patterns of the multi-model ensemble mean trends of North Atlantic 500 hPa height and precipitation match the observed trends better than for any individual model ensemble average. Moreover, the high level of reproducibility of trends among the 67 individual GOGA members of the multi-model ensemble indicates that the phase of the North Atlantic climate change

Fig. 13 Time series (1950–99) of normalized January–March (*top*) observed and (*bottom*) simulated SST over the Indian and western Pacific Ocean "warm pool" (60°E–170°E, 15°S–15°) region. The simulated SST is from a forced, historical simulation with the NCAR CSM (see text for details)
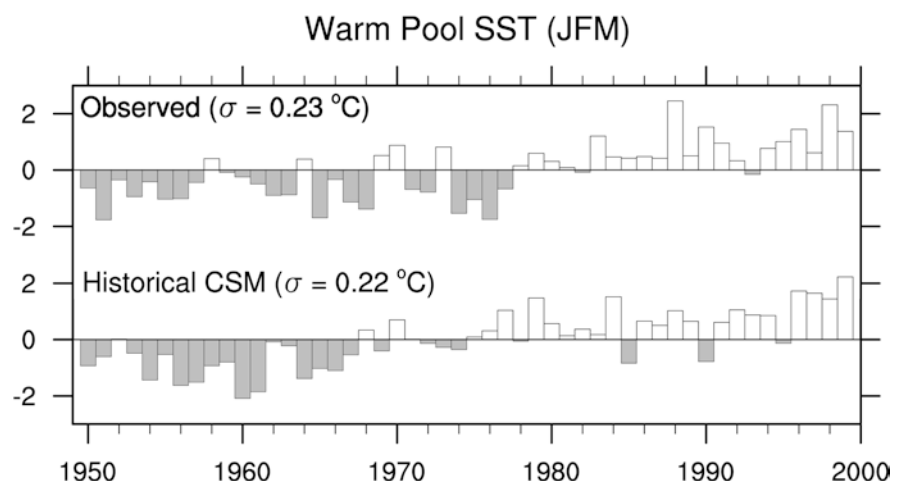
pattern was a near-deterministic response to the evolving global SSTs.

Second, we have provided a comprehensive analysis of changes in tropical SSTs and simulated precipitation patterns since 1950, including a demonstration of the high degree of reproducibility of the latter across different models. That the tropics are of fundamental importance was suggested through TOGA experiments with the NCAR AGCM, which recovered the main features of the North Atlantic climate trends evident in the global SST forcing simulations. Changes in diabatic heating anomalies associated with trends in SST and simulated rainfall over the Indian and western Pacific Oceans appear to be of primary importance, a result also supported recently in an independent modeling study by Lu et al. (2004; see also Miller et al. 2003; Sutton and Hodson 2003). They, following Peterson et al. (2002) and Lin et al. (2002), employed a simplified dynamical model forced with the spatial distribution of atmospheric diabatic heating anomalies estimated from observed circulation statistics since 1949. Using an ensemble of experiments in which the observed forcing anomalies were prescribed only over the tropics, they concluded that the trend in North Atlantic climate "can largely be explained as a hemispheric planetary wave response to forcing in the Indo-Pacific region". That such sensitivity is characteristic of different climate models was suggested through an empirical analysis that related rainfall variations over the Indian Ocean to circulation anomalies over the North Atlantic. For all four AGCMs employed in this study, enhanced rainfall over the tropical Indian Ocean produced a North Atlantic height anomaly pattern that projected onto the positive index phase of the NAO. Dynamical evidence for such a link across models is presented in our companion study.

Third, given the aforementioned results, assessing the realism of the simulated changes in Indo-Pacific rainfall was of principal importance. Through comparisons with observational records of rainfall from tropical stations throughout the region, we have shown that the simulated precipitation trends are consistent, at least in sign, with observed station trends, although the latter are highly uncertain. Moreover, independent analyses of observed, gridded rainfall anomalies appear to further confirm the simulated tropical rainfall trends over the western Pacific portion of the warm pool since 1950 (see Deser et al. 2004), and comparisons to historical simulations with fully coupled ocean-atmosphere models suggest the amplitude of the simulated rainfall anomalies is not exaggerated by the lack of an interactive ocean.

4.2 Discussion

An outstanding question regarding our simulations is whether or not the stratosphere plays a primary role in the North Atlantic tropospheric climate change since 1950. This question is especially relevant in view of the ongoing debate on whether the tropospheric NAO trend in recent decades is attributable to natural ocean-atmosphere coupled variability, or whether it is related to human-induced reductions in stratospheric ozone and/or increases in GHG concentrations (Gillett et al. 2003). The first order effect of both the observed ozone and GHG forcing changes is to enhance the meridional temperature gradient in the lower stratosphere, via radiative cooling of the polar region during winter. The dynamical adjustment to this involves an enhancement of the vertical shear of zonal wind at the middle latitude tropopause, which then strengthens the stratospheric vortex through positive dynamical feedbacks (e.g., Hartmann et al. 2000; Shindell et al. 2001; Ambaum and Hoskins 2002). It has been hypothesized, furthermore, that a stronger stratospheric polar vortex forces a tropospheric response that projects strongly onto the positive index phase of the NAO (e.g., Shindell et al. 1999; Hartmann et al. 2000; Kindem and Christiansen 2001), although the physical mechanisms are not entirely clear (Thompson et al. 2003). According to this paradigm, then, the forcing of recent trends in North Atlantic tropospheric climate fundamentally involves interactions between the stratosphere and the troposphere.

Our results offer another explanation for the observed changes, one that principally involves tropospheric processes alone. Furthermore, we provide evidence below that the recent observed trend toward a stronger NH stratospheric vortex during boreal winter can itself be reconciled with tropospheric forcing.

It is well known that the stratosphere and troposphere are strongly coupled during northern winter (e.g., Baldwin et al. 1994; Perlwitz and Graf 1995, 2001; Kitoh et al. 1996; Kodera et al. 1996), due largely to the vertical propagation of planetary waves from the troposphere into the stratosphere. It has been demonstrated, moreover, that the NH polar stratospheric circulation in recent decades has varied on interannual time scales with the flux of wave energy transmitted upward from the troposphere, and that these flux changes have been associated with changes in structure of the tropospheric stationary waves. In particular, Salby and Callaghan (2002) have demonstrated that the tropospheric circulation anomalies associated with the positive index state of the NAO (and the NH Annular Mode; Thompson et al. 2000) lead to occurrences of strong polar vortex winters via reductions in the tropospheric wave flux driving of the stratospheric meridional mass circulation. This is not to say that stratospheric feedbacks might not further modify the tropospheric structure (e.g., Baldwin and Dunkerton 2001; Perlwitz and Graf 2001; Black and McDaniel 2003), but the principal source for the stratospheric variability is the variability in tropospheric wave driving (see also Andrews et al. 1987).

Linear Trend 50hPa Z (JFM) 1950-99

Tropical SST Forcing (m 50yr⁻¹)
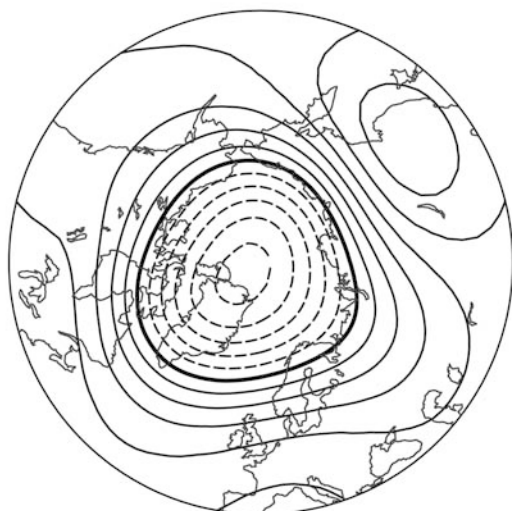
Empirical Sensitivity 50hPa Z (DJFM)

CCM3 (2400) (m)

Fig. 14 (*Top*) the linear trend (1950–99) of January–March 50 hPa ensemble mean height from the NCAR CCM3 TOGA simulation. The contour increment is 15 m per 50 years. (*Bottom*) multiple linear regression patterns for CCM3 of the winter 50 hPa height anomalies associated with a +10 mm day⁻¹ monthly averaged rainfall anomaly over the Indian Ocean centered at 70°E, 7°S (see text for details). The number of winter (December–March) months used in the calculation is indicated in *parentheses*. The contour increment is 15 m. In both panels, negative values are *dashed* and the zero contour is given by the *thick black line*

It is thus reasonable to suppose that changes in the tropospheric stationary wave structure on long time scales would also force long time scale changes in the stratospheric circulation. It is accordingly notable that the CCM3 TOGA experiments simulate not only a po-

sitive tropospheric NAO index trend, but also a trend toward a stronger stratospheric polar vortex during JFM (Fig. 14) that is qualitatively consistent with that observed (e.g., Randel and Wu 1999; Thompson et al. 2000). This is the case even though the stratosphere is not particularly well resolved in the 18-level CCM3; moreover, it argues that an important fraction of the observed height change pattern (1950–1999) from the surface through the lower stratosphere is recoverable from tropical SST forcing alone.

Additional evidence to suggest the importance of tropospheric processes in driving both the tropospheric and stratospheric height trends comes from an extension of the empirical analysis of the tropospheric sensitivity of CCM3 (Fig. 11) to lower stratospheric levels (Fig. 14, lower panel). This result demonstrates a stronger stratospheric vortex occurs on monthly time scales in conjunction with enhanced Indian Ocean diabatic heating, without any explicit requirement for SST forcing. Furthermore, in the dynamical experiments presented in our companion paper, we analyze the transient atmospheric adjustment to prescribed Indian Ocean warming and conclude that the North Atlantic tropospheric circulation changes arise as part of a hemispheric planetary wave response, consistent with the interpretation of Lu et al. (2004). Moreover, the nature of the simulated changes in tropospheric structure match closely the observed stationary wave structure shown by Salby and Callaghan (2002) to have been important for the tropospheric wave driving of interannual variations in the strength of the stratospheric polar vortex in recent decades.

Finally, it could nonetheless be true that both the tropospheric and stratospheric circulation trends over the last half of the twentieth Century have been tied to increased GHG concentrations, even though the source for our attribution work has been AGCM simulations using fixed atmospheric chemistry. This is because the history of prescribed SSTs likely contains an anthropogenic component, including the observed warming of Indian Ocean surface waters (e.g., Knutson et al. 1999). That the close match to the observed warm pool SST time series since 1950 by the historical CSM simulation (Fig. 13) cannot be attributed to natural variability in the coupled model is demonstrated in Hoerling et al. (2004), where we also highlight similar behavior in historical simulations with other coupled models. Thus, the results presented herein do not discount the existence of an indirect greenhouse effect through the dynamical response to the tropical ocean changes of the last half-century.

References

Alexander MA (1992) Midlatitude atmosphere-ocean interaction during El Niño. Part II: the Northern Hemisphere atmosphere. J Clim 5: 959–972

Ambaum MH, Hoskins BJ (2002) The NAO troposphere-stratosphere connection. J Clim 15: 1969–1978

Andrews DG, Holton J, Leovy CB (1987) Middle atmosphere dynamics, Academic Press, San Diego, CA, USA pp 489

Baldwin MP, Dunkerton TJ (2001) Stratospheric harbingers of anomalous weather regimes. Science 294: 581–584

Baldwin MP, Cheng X, Dunkerton TJ (1994) Observed correlations between winter-mean tropospheric and stratospheric circulation anomalies. Geophys Res Lett 21: 1141–1144

Barsugli JJ, Battisti DS (1998) The basic effects of atmosphere-ocean thermal coupling on midlatitude variability. J Atmos Sci 55: 477–493

Black RX (2002) Stratospheric forcing of surface climate in the Arctic Oscillation. J Clim 15: 268–277

Black RX, McDaniel BA (2003) Stratosphere-troposphere interactions: case studies of the NAM. Bull Amer Meteorol Soc 84: 900

Bottomley M, Folland CK, Hsiung J, Newell RE, Parker DE (1990) Global ocean surface temperature atlas. UK Meteorological Office, Reading, UK, pp 20, and 313 plates

Boville BA, Gent PR (1998) The NCAR Climate System Model, Version One. J Clim 11: 1115–1130

Bretherton CS, Battisti DS (2000) An interpretation of the results from atmospheric general circulation models forced by the time history of the observed sea surface temperature distribution. Geophys Res Lett 27: 767–770

Cassou C, Terray L (2001) Dual influence of Atlantic and Pacific SST anomalies on the North Atlantic/Europe winter climate. Geophys Res Lett 28: 3195–3198

Cayan DR (1992a) Latent and sensible heat flux anomalies over the northern oceans: driving the sea surface temperature. J Phys Oceanogr 22: 859–881

Cayan DR (1992b) Latent and sensible heat flux anomalies over the northern oceans: the connection to monthly atmospheric circulation. J Clim 5: 354–369

Chen P, Robinson WA (1992) Propagation of planetary waves between the troposphere and stratosphere. J Atmos Sci 49: 2533–2545

Cook ER (2003) Multi-proxy reconstructions of the North Atlantic Oscillation (NAO) index: a critical review and a new well-verified winter NAO index reconstruction back to AD 1400. In: Hurrell JW, Kushnir Y, Ottersen G, Visbeck M (eds) The North Atlantic Oscillation: climatic significance and environmental impact. Geophys Monogr 134: 63–79

Czaja A, Robertson AW, Huck T (2003) The role of Atlantic ocean-atmosphere coupling in affecting North Atlantic Oscillation Variability. In: Hurrell JW, Kushnir Y, Ottersen G, Visbeck M (eds) The North Atlantic Oscillation: climatic significance and environmental impact. Geophys Monogr 134: 147–172

Deser C, Timlin MS (1997) Atmosphereocean interaction on weekly time scales in the North Atlantic and Pacific. J Clim: 393-408

Deser C, Phillips AS, Hurrell JW (2004) Pacific interdecadal climate variability: linkages between the tropics and North Pacific in boreal winter since 1900. J Clim (in press)

Ferrara JD, Mechoso CR, Robertson AW (2000) Ensembles of AGCM two-tier predictions and simulations of the circulation anomalies during winter 1997–98. Mon Weather Rev 128: 3589–3604

Feldstein SB (2000) Teleconnections and ENSO: the time scale, power spectra, and climate noise properties. J Clim 13: 4430–4440

Feldstein SB (2002) The recent trend and variance increase of the Annular Mode. J Clim 15: 88–94

Gates WL and Coauthors (1999) An overview of the results of the Atmospheric Model Intercomparison Project (AMIP I). Bull Am Meteorol Soc 80: 335–345

Gillett NP, Baldwin MP, Allen MR (2001) Evidence for nonlinearity in observed stratospheric circulation changes. J Geophys Res 106: 7891–7901

Gillett NP, Graf HF, Osborn TJ (2003) Climate change and the North Atlantic Oscillation. In: Hurrell JW, Kushnir Y, Ottersen G, Visbeck M (eds) The North Atlantic Oscillation: climatic significance and environmental impact. Geophys Monogr 134: 193–209

Greatbatch R J (2000) The North Atlantic Oscillation. Stochastic and environmental Risk Assessment 14: 213–242

Hartmann DL, Wallace JM, Limpasuvan V, Thompson DWJ, and Holton JR (2000) Can ozone depletion and greenhouse warming interact to produce rapid climate change? Proc Nat Acad Sci 97: 1412–1417

Haynes PH, Marks CJ, McIntyre ME, Shepherd TG, Shine KP (1991) On the "downward control" of extratropical diabatic circulations by eddy-induced mean zonal forces. J Atmos Sci 48: 651–678

Hoerling MP, Hurrell JW, Xu T (2001a) Tropical origins for recent North Atlantic climate change. Science 292: 90–92

Hoerling MP, Kumar A, Whitaker JS, Wang W (2001b) The midlatitude warming during 1998–2000. Geophys Res Lett 28: 755–758

Hoerling MP, Hurrell JW, Xu T, Bates GT, Phillips AS (2004) Twentieth century North Atlantic climate change. Part II: understanding the effect of Indian Ocean warming. Clim Dyn (in press)

Hurrell JW (1995) Decadal trends in the North Atlantic oscillation: regional temperatures and precipitation. Science 269: 676–679

Hurrell JW, van Loon H (1997) Decadal variations in climate associated with the North Atlantic Oscillation. Clim Change 36: 301–326

Hurrell JW, Trenberth KE (1999) Global sea surface temperature analyses: multiple problems and their implications for climate analysis, modeling, and reanalysis. Bull Am Meteorol Soc 80: 2661–2678

Hurrell JW, Kushnir Y, Ottersen G, Visbeck M (2003) An overview of the North Atlantic Oscillation. In: Hurrell JW, Kushnir Y, Ottersen G, Visbeck M (eds) The North Atlantic Oscillation: climatic significance and environmental impact. Geophysi Monograph 134: 1–35

Jones PD, Osborn TJ, Briffa KR (2001) The evolution of climate over the last millennium. Science 292: 662–667

Kalnay E, and Coauthors (1996) The NCEP/NCAR 40-year reanalysis project, Bull Am Meteorol Soc 77: 437–471

Kiehl JT, Hack JJ, Bonan GB, Boville BA, Williamson DL, Rasch PJ (1998) The National Center for Atmospheric Research Community Climate Model: CCM3. J Clim 11: 1131–1149

Kindem IT, Christiansen B (2001) Tropospheric response to stratospheric ozone loss. Geophys Res Lett 28: 1547–1550

Kitoh A, Doide H, Kodera K, Yukimoto S, Noda A (1996) Interannual variability in the stratospheric- tropospheric circulation in a coupled ocean-atmosphere GCM. Geophys Res Lett 23: 543–546

Knutson TR, Delworth TL, Dixon KW, Stouffer RJ (1999) Model assessment of regional surface temperature trends (1949–1997). J. Geophys Res 104: 30981–30996, DOI 1999JD900965

Kodera K, Chiba M, Koide H, Kitoh A, Nikaidou Y (1996) Interannual variability of the winter stratosphere and troposphere in the Northern Hemisphere. J Meteorol Soc Jpn 74: 365–382

Kumar A, Hoerling MP (1995) Prospects and limitations of seasonal atmospheric GCM predictions. Bull Am Meteorol Soc 76: 335–345

Kushnir Y, Robinson WA, Bladé I, Hall NMJ, Peng S, Sutton RT (2002) Atmospheric GCM response to extratropical SST anomalies: synthesis and evaluation. J Clim 15: 2233–2256

Leith CE (1973) The standard error of time-averaged estimates of climatic means. J Appl Meteorol 12:1066–1069

Lin H, Derome J, Greatbatch RJ, Peterson KA, Lu J (2002) Tropical links of the Arctic Oscillation. Geophys Res Lett 29, DOI 10.1029/2002GL015822

Lu J, Greatbatch RJ, Peterson KA (2004) On the trend in Northern Hemisphere winter atmospheric circulation during the last half of the twentieth Century. J Clim (in press)

Madden RA (1976) Estimates of the natural variability of time-averaged sea-level pressure. Mon Weather Rev 104: 942–952

Marshall J, Kushnir Y, Battisti D, Chang P, Czaja A, Dickson R, Hurrell J, McCartney M, Saravanan R, Visbeck M (2001) North Atlantic climate variability: phenomena, impacts and mechanisms. Int J Climatol 21: 1863–1898

Mehta V, Suarez M, Manganello JV, Delworth TD (2000) Oceanic influence on the North Atlantic Oscillation and associated Northern Hemisphere climate variations: 1959–1993. Geophys Res Lett 27: 121–124

Miller AJ, Zhou S, Yang S.-K (2003): Relationship of the Arctic and Antarctic Oscillations to the outgoing longwave radiation. J Clim 16: 1583–1592

Osborn TJ (2004) The winter North Atlantic Oscillation: the roles of internal variability and greenhouse gas forcing. Clim Dyn (in press)

Osborn TJ, Briffa KR, Tett SFB, Jones PD, Trigo RM (1999) Evaluation of the North Atlantic oscillation as simulated by a climate model. Clim Dyn 15: 685–702

Parker DE, Jones PD, Folland CK, Bevan A (1994) Interdecadal changes of surface temperature since the late nineteenth century. J Geophys Res 99: 14373–14399

Pegion P, Suarez M, Schubert S (2001) An analysis of the causes of differences in circulation patterns during the El Niño winters of 1983 and 1998. Proc 26th Annual Climate Diagnostics and Prediction Workshop, La Jolla, CA. National Oceanic and Atmospheric Administration

Peng S, Robinson WA, Li S (2003) Mechanisms for the NAO responses to the North Atlantic SST tripole. J Clim 15: 1987–2004

Perlwitz J, Graf H-F (1995) The statistical connection between tropospheric and stratospheric circulation of the Northern Hemisphere in winter. J Clim 8: 2281–2295

Perlwitz J, Graf H-F (2001) Troposphere-stratosphere dynamic coupling under strong and weak polar vortex conditions. Geophys Res Lett 28: 271–274

Peterson KA, Greatbatch RJ, Lu J, Lin H, Derome J (2002) Hindcasting the NAO using diabatic forcing of a simple AGCM. Geophys Res Lett 29: DOI 10.1029/2001GL014502

Polvani LM, Kushner PJ (2002) Tropospheric response to stratospheric perturbations in a relatively simple general circulation model. Geophy Res Lett 29: 1114 DOI 10.1029/2001GL014284

Pozo-Vázquez D, Esteban-Parra MJ, Rodrigo FS, Castro-Díez Y (2001) The association between ENSO and winter atmospheric circulation and temperature in the North Atlantic region. J Clim 14: 3408–3420

Rajagolapan B, Kushnir Y, Tourre Y (1998) Observed decadal midlatitude and tropical Atlantic climate variability. Geophys Res Lett 25: 3967–3970

Randel WJ, Wu F (1999) Cooling of the Arctic and Antarctic polar stratospheres due to ozone depletion. J Clim 12: 1467–1479

Rayner NA, Horton EB, Parker DE, Folland CK, Hackett RB (1996) Version 2.2 of the Global Sea-Ice and Sea Surface Temperature data set, 1903–1994. CRTN 74, pp. 21 plus figures

Rayner NA, Parker DE, Horton EB, Folland CK, Alexander LV, Rowell DP (2003) Global analyses of SST, sea ice and night marine air temperature since the late nineteenth century. J Geophys Res DOI 10.1029/2002JD002670

Reynolds RW (1988) A real-time global sea surface temperature analysis. J Clim 1: 75–86

Reynolds RW, Smith TM (1994) Improved global sea surface temperature analyses using optimum interpolation. JClim 7: 929–948

Reynolds RW, Rayner NA, Smith, TM, Stokes DC, Wang W (2002) An improved in situ and satellite SST analysis for climate. J Clim 15: 1609–1625

Robertson AW, Mechoso CR, Kim YJ (2000) The influence of Atlantic sea surface temperature anomalies on the North Atlantic Oscillation. J Clim 13: 122–138

Rodwell MJ, Rowell DP, Folland CK (1999) Oceanic forcing of the wintertime North Atlantic Oscillation and European climate. Nature 398: 320–323

Roeckner E and Coauthors (1996) The atmospheric general circulation model ECHAM4: model description and simulation of present-day climate. Max Planck Institut fur Meteorolologiem Report No 218, Hamburg, Germany, pp 90

Rogers JC, van Loon H (1979) The seasaw in winter temperature between Greenland and Northern Europe, Part II: some oceanic and atmospheric effects in middle and high latitudes. Mon Weather Rev 107: 509–519

Salby ML, Callaghan PF (2002) Interannual changes of the stratospheric circulation: relationship to ozone and tropospheric structure. J Clim 24: 3673–3685

Saravanan R, Giannini A, Chang P, and Ji L (2002) Estimating potential predictability associated with tropical Atlantic SST anomalies. In: Legler D (ed) Proceedings of the US. CLIVAR Atlantic conference. US CLIVAR Office, Washington DC USA pp 91–93

Schmutz C, Luterbacher J, Gyalistras D, Xoplaki E, Wanner H (2000) Can we trust proxy-based NAO index reconstructions? Geophy Res Lett 27: 1135–1138

Schneider EK, Bengtsson L, Hu Z-Z (2003) Forcing of Northern Hemisphere climate trends. J Atmos Sci 60: 1504–1521

Schubert SD, Suarez MJ, Pegion PJ, Koster RD, Bacmeister JT (2002) Causes of long-term drought in the United States Great Plains. J Clim 17: 485–503

Shindell DT, Miller RL, Schmidt G, Pandolfo L (1999) Simulation of recent northern winter climate trends by greenhouse-gas forcing. Nature 399: 452–455

Shindell DT, Schmidt GA, Miller RL, Rind D (2001) Northern hemisphere winter climate response to greenhouse gas, ozone, solar, and volcanic forcing. J Geophys Res 106: 7193–7210

Smith TM, Reynolds RW, Livezey RE, Stokes DC (1996) Reconstruction of historical sea surface temperatures using empirical orthogonal functions. J Clim 9: 1403–1420

Stephenson DB, Pavan V (2003) The North Atlantic Oscillation in coupled climate models: a CMIP1 evaluation. Clim Dyn 20: 381–399

Stephenson DB, Pavan V, Bojariu R (2000) Is the North Atlantic Oscillation a random walk? Int J Climatol 20:1–18

Sutton RT, Hodson DLR (2003) The influence of the ocean on North Atlantic climate variability 1871–1999. J Clim 16: 3296–3313

Sutton RT, Norton WA, Jewson SP (2001) The North Atlantic Oscillation - what role for the ocean? Atmos Sci Lett DOI 10.1006/asle.2000.0018

Thompson DWJ, Wallace JM, Hegerl GC (2000) Annular modes in the extratropical circulation, Part II: trends. J Clim 13: 1018–1036

Thompson DWJ, Lee S, Baldwin MP (2003) Atmospheric processes governing the Northern Hemisphere Annular Mode/ North Atlantic Oscillation. In: Hurrell JW, Kushnir Y, Ottersen G, Visbeck M (eds) The North Atlantic Oscillation: climatic significance and environmental impact. Geophys Monogr 134: 81–112

Trenberth KE, Caron JM (2000) The Southern Oscillation revisited: sea level pressures, surface temperatures and precipitation. J Clim 13: 4358–4365

Trenberth KE, Branstator GW, Karoly D, Kumar A, Lau N.-C, Ropelewski C (1998) Progress during TOGA in understanding and modeling global teleconnections associated with tropical sea surface temperatures. J Geophys Res 103: 14291–14324

Venzke S, Allen MR, Sutton RT, Rowell DP (1999) The atmospheric response over the North Atlantic to decadal changes in sea surface temperatures. J Clim 12: 2562–2584

Visbeck M, Chassignet EP, Curry RG, Delworth TL, Dickson RR, Krahmann K (2003) The ocean's response to North Atlantic Oscillation variability. In: Hurrell JW, Kushnir Y, Ottersen G, Visbeck M (eds) The North Atlantic Oscillation: climatic significance and environmental impact. Geophys Monogr 134: 113–146

Vose RS, Schmoyer RL, Steurer PM, Peterson TC, Heim R, Karl TR, Eischeid JK (1992) The Global Historical Climatology Network: Longterm monthly mean temperature, precipitation, sea level pressure, and station pressure data. ORNL/CDIAC-53, NDP-041. Carbon Dioxide Analysis Center, pp 100

Wanner H, Brönnimann S, Casty C, Gyalistras D, Luterbacher J, Schmutz C, Stephenson DB, Xoplaki E (2001) North Atlantic Oscillation - concepts and studies. Survey Geophys 22: 321–381

Weickmann KM, Lussky GL, Kutzbach JE (1985) Intraseasonal (30–60 day) fluctuations of outgoing longwave radiation and 250 mb streamfunction during northern winter. Mon Weather Rev 113: 941–961

Woodruff SD, Slutz RJ, Jenne RL, Steurer PM (1987) A Comprehensive Ocean-Atmosphere Data Set. Bull Am Meteorol Soc 68: 1239–1250

Wunsch C (1999) The interpretation of short climate records, with comments on the North Atlantic Oscillation and Southern Oscillations. Bull Am Meteorolol Soc 80: 245–255

Xie S-P, Tanimoto Y (1998) A pan-Atlantic decadal climate oscillation. Geophys Res Lett 25: 2185–2188

Zhou S, Miller AJ, Wang J, Angell JK (2001) Trends of NAO and AO and their associations with stratospheric processes. Geophys Res Lett 28: 4107–4110